NEW SMALL IMPACT CRATERS IN HIGH RESOLUTION HIRISE IMAGES - IV. B. A. Ivanov[1], H. J. Melosh[2], A. S. McEwen[3], and the HiRISE team, [1]Institute for Dynamics of Geospheres, RAS, 119334, Moscow, Russia, baivanov@idg.chph.ras.ru, [2]Dep. of Earth and Atmospheric Sciences, Purdue University, West Lafayette IN 47907 (jmelosh@purdue.edu) [3]University of Arizona, Department of Planetary Sciences, Tucson, AZ, 85721.

Introduction: Repetitive imaging of Mars revealed potential "new" impact sites [1, 2]: impact craters with known time periods of formation. To date, about 300 "new" impact craters are found mostly in dusty areas [2, 5-8]. Previously W. Hartmann [3] proposed a lunar-derived Martian chronology based on an atmospheric shielding model [4]. The current presentation further evaluates the correctness of the Moon/Mars cratering comparison for small young (<10 years) craters and density estimates of Martian projectiles.

Single craters: We present a simple model of atmospheric shielding for the modern Martian atmosphere. Analytical models for atmospheric deceleration and ablation of small bodies without fragmentation - iron, ordinary (OC) and carbonaceous (CC) chondrites, solid ice - with coefficients from [9] are used to estimate the size-frequency distribution (SFD) of small Martian single craters. The input masses are taken as random numbers following a power law consistent with the crater SFD in the lunar regolith [10] $N_{>D} \sim D^{-2.93}$. We found that Hartmann [3] uses an exponent of -3.2 in his estimates The -2.93 exponent better fits small crater and terrestrial bolide records. [13].

For the Monte-Carlo model the impact velocity is randomly taken from the distribution of "astorb.dat" data [14] (weighted by impact probability). The impact angle is randomly chosen from a standard distribution that peaks at 45°. For the same randomly chosen projectile mass the model computes crater sizes on the Moon, atmosphere-less Mars, deceleration only, and deceleration+ablation in the current Martian atmosphere. The "dry sand" (gravity dominated) scaling law is used to estimate crater sizes. Final craters sizes are sorted in standard bins with a step of $2^{0.5}$. In further work we plan to test the "strength scaling" for Mars.

Preliminary results. Fig. 1 compares the model derived SFD for OC, CC and solid ice (as a first order proxy for cometary materials. The SFD is not affected by ablation for OC, but significantly changes the SFD for CC and ice. Atmospheric deceleration dramatically decreases the impact velocity as well as the standard deviation of impact velocity for a given crater diameter bin (Fig. 2). For the average entry velocity of ~10.8 kms^{-1} craters of ≤10 m in diameter are formed at ~5 kms^{-1}. Ablation can remove 10 to 30% of the initial projectile mass. For ice projectiles ablation can remove ~50% of mass even for a 100 m diameter crater.

Fig.3 shows an example of the model comparison with the real single crater SFD. The compilation [2] of newer findings is used to select single craters formed after 2005. Inclusion of atmospheric shielding is essential for all craters below ~50 m in diameter. The R-plot deficiency due to the atmosphere is a factor of 2 to 3 at D~10 m. This result will be used in future work with various mixtures of different kinds of projectiles. However, the OC non-porous model in Fig.3 seems to explain the flat (in R-plots) SFD for single craters from 10-50 m diameter.

Pairs of craters: The distance between pair of craters in binary impacs (42 cases of 270 total impacts) and between largest craters in some cluster impacts (47 cases of total 83 clusters) offers the possibility of estimating the density of fragmented projectiles [11]. With the accumulated statistics for "new" craters we can try a statistical approach. Assuming tentatively the value of separation for the vertical impact we can construct a statistical model of the distribution of separation distances for a random entry angle and random orientation of fragment directions after the breakup. We numerically computed several (seven) distributions with various nominal separation distances (for a vertical impact) from 8 to 48 m and weighted the number of cases with each nominal separation value to fit the observed distribution of distances between pairs of craters. The single value of the nominal separation distance is defined by a combination of the projectile density and the breakup altitude. The same nominal separation corresponds to projectiles with a specific combination of strength and density but not define them separately.

Fig. 4 illustrates the comparison of the model variant with real observations. The separation distances are binned in logarithmically equal intervals, where the upper limit is a factor of $2^{0.5}$ larger than the lower limit. The maximum is located in the bin where the separation distance is from 22.6 to 32 m.

The separation distance depends on the separation coefficient c_T defining the value of the transverse separation velocity (v_T) through the projectile velocity (v), and the ratio of projectile and atmospheric density at the breakup altitude [11]:

$$v_T = c_T\, v\, (\rho_{atm}/\rho_{proj})^{0.5}$$

The separation distance for vertical impacts in the range of ~35 to ~50 m corresponds (providing the optimum breakup altitude at 22 km [11]) to a density of ~1150 kgm^{-3} and a separation coefficient c_T ~ 0.9 [12]. If one assumes that the separation coefficient is about 1.5 [11], the most probable projectile density rises to ~2400 kgm^{-3}.

Conclusions: The relatively wide spread of projectile fragments in the Martian atmosphere suggests low density objects in standard models. However, the single crater SFD is well reproduced with "normally" dense ordinary chondrites. The separation distance of pairs of craters may be tentatively reproduced with "dense" meteoroids if the separation coefficient is larger than in available models. More work is needed to construct a clear picture. Increased HiRISE/CTX observational statistics would result in a significant improvement of our models.

References: [1] Malin M.C. et al. (2006) *Science, 314*, 1573-1577. [2] Daubar I. et al. (2013) *Icarus 225*, 506-516. [3] Hartmann W.K. (2005) *Icarus 174*, 294-320. [4] Popova O. P. et al. (2003) *MAPS 38*, 905-925. [5] Ivanov B.A., H.J. Melosh, and A.S. McEwen (2008) *LPS XXXIX*, Abstract #1402. [6] Ivanov B.A., H.J. Melosh, and A.S. McEwen (2008) *3d EPSC (Münster)*, Abstract # EPSC2008-A-00340. [7] Ivanov B.A., H.J. Melosh, and A.S. McEwen (2009) *LPS XXXX*, Abstract #1410. [8] Ivanov B.A., H.J. Melosh, and A.S. McEwen (2010) *LPS 41st*, Abstract #2020. [9] Ceplecha Z. (1987) *Bull. Astron. Inst. of Czechoslovakia, 38*, 222-234. [10] Shoemaker E.M.et al. (1970) *Science 167*, 452-455. [11] Passey Q.R. and H.J. Melosh (1980) *Icarus 42*, 211-233. [12] Artem'eva N.A. and V.V. Shuvalov (1996) *Shock Waves 5*, 359-367. [13] Ivanov B. A. (2006) Icarus 183, 504-507. [14] http://www.naic.edu/~nolan/

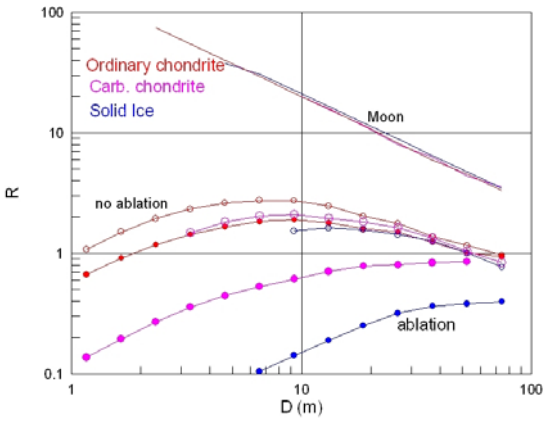

Fig. 1. R-plot for model SFDs for different material of projectiles. All data are scaled to give the same lunar crater SFD.

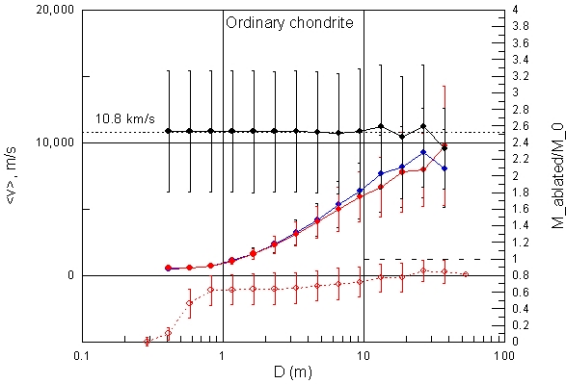

Fig. 2. Entry velocity (black circles) and impact velocities (blue curve – no ablation, red curve – with ablation, all referred to left vertical scale) for OC projectiles, the lower dashed red curve shows ablation (initial to impact mass ratio, right vertical scale). All error bars show 1σ value.

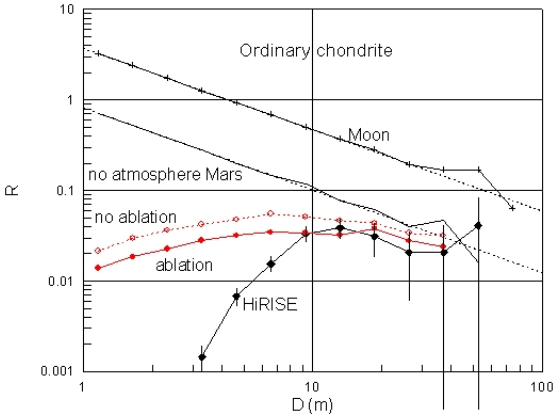

Fig. 3. Model SFD for OC projectiles with ablation (solid red curve) and without ablation (dashed red curve) in comparison with the single crater HiRISE SFD formed after 2005. The SFD downturn below 10 m is probably dominated by resolution of CTX images used to discover new impact sites [2].

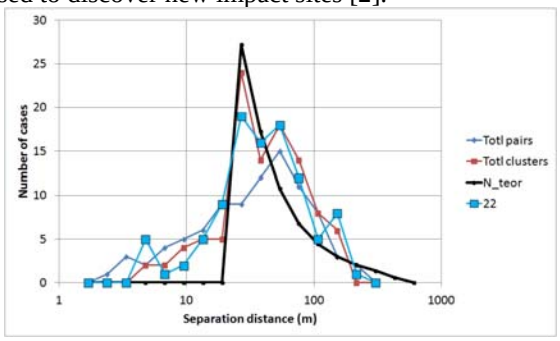

Fig. 4. The distribution of pair separation distances at the surface. Black curve is the model, red curve is for clusters, and cyan curve is for crater pairs. The cyan curve with square markers is an altitude correction assuming 22 km breakup altitude.